Volume 19, No 1 | International Journal of Radiation Research, January 2021

Ionizing radiation induces ferroptosis in splenic lymphocytes of mice

X. Zhang[1,2,3*], H. Liu[1*], X. Xing[1], M. Tian[1], X. Hu[1], F. Liu[4,5,6], J. Feng[1], S. Chang[1], P. Liu[3], H. Zhang[1,2]

[1]*Department of Nuclear Science and Engineering, Nanjing University of Aeronautics and Astronautics, Nanjing, Jiangsu, P.R. China*
[2]*Jiangsu Key Laboratory for Biomaterials and Devices, Southeast University, Nanjing, Jiangsu, P.R. China*
[3]*Key Laboratory of Nuclear Technology Application and Radiation Protection in Astronautics, Ministry of Industry and Information Technology, Nanjing, P.R. China*
[4]*Department of Head and Neck Surgery, Jiangsu Cancer Hospital, Nanjing, Jiangsu, P.R. China*
[5]*Jiangsu Institute of Cancer Research, Nanjing Medical University, Nanjing, Jiangsu, P.R. China*
[6]*Affiliated Cancer Hospital, Nanjing, Jiangsu, P.R. China*

[Downloaded from ijrr.com on 2026-11-10]

[DOR: 20.1001.1.23223243.2021.19.1.12.3]
[DOI: 10.29252/ijrr.19.1.99]

► ***Original article***

***Corresponding authors:**
Xiaohong Zhang, PhD.,
E-mail:
zhangxiaohong@nuaa.edu.cn

Fangzhou Liu, M.D.
***E-mail:** zyfz1103@163.com*

Revised: February 2020
Accepted: February 2020

Int. J. Radiat. Res., January 2021; 19(1): 99-111

DOI: 10.29252/ijrr.19.1.99

ABSTRACT

Backgrounds: It remains unclear whether radiation-induced haemorrhage in the spleen causes iron accumulation, and subsequently, ferroptosis in splenic lymphocytes. In this study, we investigated the occurrence of ferroptosis in splenic lymphocytes of gamma-irradiated mice. ***Materials and Methods:*** Mice were subjected to gamma radiation from a ^{137}Cs source. Iron, Ferroportin 1, and iron regulatory protein (IRP) levels in the spleen, and serum iron and hepcidin levels in the blood were measured to study the change in iron metabolism of the irradiated spleen. After Ferrostatin 1/LDN193189 was intraperitoneally injected into mice post-irradiation, the viability of splenic lymphocytes and the splenic index were evaluated to investigate the mechanism of damage induction in splenic lymphocytes. The survival rate of mice was evaluated to identify the radiation mitigator based on the inhibition of ferroptosis. ***Results:*** Iron accumulation (up to 0.62 g/g) observed in the spleen of irradiated mice was due to haemorrhage-based haemosiderin. The iron accumulation triggered the IRP-ferroportin 1 axis to increase the level of serum iron to 121.65 mmol/l. LDN193189 was used to demonstrate that the iron accumulation decreased the viability of splenic lymphocytes in irradiated mice, which was subsequently demonstrated to attribute to ferroptosis with the use of Ferrostatin 1 and through detection of ferroptosis-related parameters. The survival rate of irradiated mice was improved upon Ferrostatin-1 (60% with a duration of 120 days) or LDN193189 (40% for the same duration) treatment. ***Conclusion:*** Radiation-induced haemorrhage causes ferroptosis in splenic lymphocytes, and anti-ferroptosis is a potential strategy to alleviate immune damage in hematopoietic acute radiation sickness.

Keywords: *Hematopoietic acute radiation sickness, iron metabolism, iron accumulation, splenic lymphocyte, ferroptosis.*

INTRODUCTION

As nuclear technologies are used worldwide, radiation/nuclear accidents may occur frequently. Victims of unplanned radiation exposure (1-10 Gy) show hematopoietic acute radiation sickness. Infection is one of the lethal symptoms in hematopoietic acute radiation sickness. The spleen is the largest peripheral immune organ. Exposure to high radiation dose

causes severe reduction in spleen weight, which relates to the immunosuppression in hematopoietic acute radiation sickness [1-3]. Elucidation of mechanisms of radiation-induced immune damage in the spleen is therefore particularly crucial in finding the effective treatment for hematopoietic acute radiation sickness.

Earlier studies on radiation-induced alterations in the immune function of the spleen have concentrated on the change in the frequency and ultrastructure of spleen mast cells [4] and the suppression of antibody synthesis in splenic cells [5]. Expression of the cytokines interleukin-1 alpha and beta has been reported to increase in splenic cells of irradiated mice [6, 7]. As a radiosensitive mature blood cell, the lymphocyte count decreases at the early stage after irradiation. Lymphocyte-mediated specific immunity is the second line of defense in the immune system. Given that the lymphocyte reside and proliferate in the spleen, the research on radiation-induced injury to splenic lymphocytes has gathered interest. It has been generally accepted that radiation-induced cell death in splenic lymphocytes occurs by apoptosis [8], which is caused by accumulation of DNA damage in cells [9]. However, ionizing radiation induces five types of cell death: necrosis, apoptosis, autophagy, mitotic catastrophe, and senescence [10]. The diversity in the forms of radiation-induced cell death indicates that mechanisms associated with radiation-induced cell death in splenic lymphocytes can be very complicated. We therefore reasonably speculated that irradiated splenic lymphocytes can undergo other forms of cell death exist besides apoptosis.

Iron is an essential micronutrient for many cellular processes, including DNA synthesis, hemoglobin synthesis, oxidative cell metabolism, and cell respiration [11]. Although iron plays a vital role in sustaining life, the body is highly sensitive to iron concentration. The iron metabolism system has therefore been developed to regulate the iron concentration elaborately [12]. Iron accumulation exceeding the regulatory capacity of iron metabolism will show cellular toxicity via the Fenton reaction and iron-mediated lipid peroxidation [13]. The highest form of iron-mediated cellular toxicity is ferroptosis, which is an iron-dependent form of cell death driven by accumulation of lipid-based reactive oxygen species (ROS), activation of enzymes for lipid peroxidation [14, 15], and depletion of glutathione peroxidase 4 (GPX4) [16-18]. There are two pathways for the induction of ferroptosis. The first is canonical induction, which is through inactivation of the major protective mechanism of the membrane against peroxidation damage [19]. For example, under insufficiency or dysfunction of GPX4, phosphatidylethanolamine binding protein 1/15 -lipoxygenase complex induces ferroptosis by the generation of 15-HPETE-PE [20]. The second is non-canonical induction, which is liable iron pool (LIP)-related [19]. For example, the addition of iron-bound transferrin [16] or ferric ammonium citrate [21] has been shown to potentiate erastin-induced ferroptosis. *Iron-response element-binding protein 2* (*IREB2*) encoding a master regulator of iron metabolism has been identified as a high-confidence gene for erastin-induced ferroptosis in both HT-1080 and Calu-1 cells, and silencing of *IREB8* has conferred protection against erastin-induced ferroptosis [21]. Viscus bleeding is an essential sign of hematopoietic acute radiation sickness. Erythrocytes are iron-rich cells, and viscus bleeding means that erythrocytes enter the tissue that will be engulfed and degraded by macrophages. The corresponding heme will be subsequently decomposed into ferrous iron, biliverdin, and carbon monoxide with the catalysis of heme oxygenase-1(HO-1) [22]. If HO-1 is deficient, the accumulative hemes will combine with proteins to form hemosiderin. No matter what the condition of HO-1 is, severe hemorrhage in the viscera can cause increased iron level. The spleen is not only an immune organ but also a viscus for blood storage. Once radiation-induced bleeding occurs in the spleen, the possibility of iron accumulation in the spleen is increased. Based on the abovementioned theories, we hypothesized that ionizing radiation induces iron accumulation in the spleen, and this kind of iron accumulation injures splenic lymphocytes via ferroptosis. In

[Downloaded from ijrr.com on 2026-11-10]
[DOR: 20.1001.1.23223243.2021.19.1.12.3]
[DOI: 10.29252/ijrr.19.1.99]

this study, we demonstrated that gamma radiation causes an increase in the iron content of the spleen, and injures splenic lymphocytes via ferroptosis in a mouse model.

MATERIALS AND METHODS

Animals

Ma1e ICR mice were purchased from the Animal Center of Nantong University (Nantong, Jiangsu, China). All of the mice used were at approximately 8-10 weeks of age. The mice were housed in cages in an animal room for one week under the following conditions: the temperature at 23±2 °C, the relative humidity at 55±15%, 12 air changes per hour, and a 12-h light-dark cycle. The experimental protocol involving animals was reviewed and approved by the Institutional Animal Care and Use Committee of Nanjing University of Aeronautics and Astronautics. The Guidelines for the Care and Use of Laboratory Animals were strictly followed by all the studies on animals.

Radiation treatments and reagent administrations

Mice placing in ventilated plexiglass cages received whole-body irradiation with a ^{137}Cs source (Hopewell Designs Inc., Alpharetta, GA, USA). The absorbed doses were 0, 4, 8, and 10 Gy at a dose rate of 2 Gy/min. The skin-source distance was 50 cm. The dosimetry was performed with a 0.6 cm^3 Farmer Ionization Chamber (Type 30010) which was connected to a dosimeter (Unidos, PTW-Freiburg, Freiburg, Germany). The chamber was placed parallel to the plexiglass cage for irradiation.

When the iron metabolism and ferroptosis-related parameters were studied, mice were randomly divided into the 0 Gy group and radiation group. When LDN193189 (APExBIO, Shanghai, China)/ Ferrostatin-1 (APExBIO)/deferoxamine (DFO; Sigma Chemical, St. Louis, MO, USA) was administered intraperitoneally, mice were randomly divided into the 0 Gy group, 0 Gy + reagent group, radiation group, and radiation + reagent group (figure 1). LDN193189/DFO was dissolved in sterile distilled water pretreated to 37 °C. Ferrostatin-1 was dissolved in 0.01% of DMSO (in 0.9% of saline) under ultrasonic treatment at 37 °C. The solvents were included in the 0 Gy group/radiation group. Three mg/kg of LDN193189 [23] was injected into mice at time points of 24 and 48 h post-irradiation. The dose of of Ferrostatin-1 (2 mg/kg), adjusting according to Sui *et al.* [24], was injected at a time point of 72 h post-irradiation (24). The dose of DFO (210 mg/kg), adjusting according to Yao *et al.* [25], was injected once a day for 6 days post-irradiation. Mice in the 0 Gy group or treated with reagent alone were sham-irradiated. Each group included six mice except the section of survival assessment that included 10 mice in each group. Five hundred and eighty-four mice were used in this study.

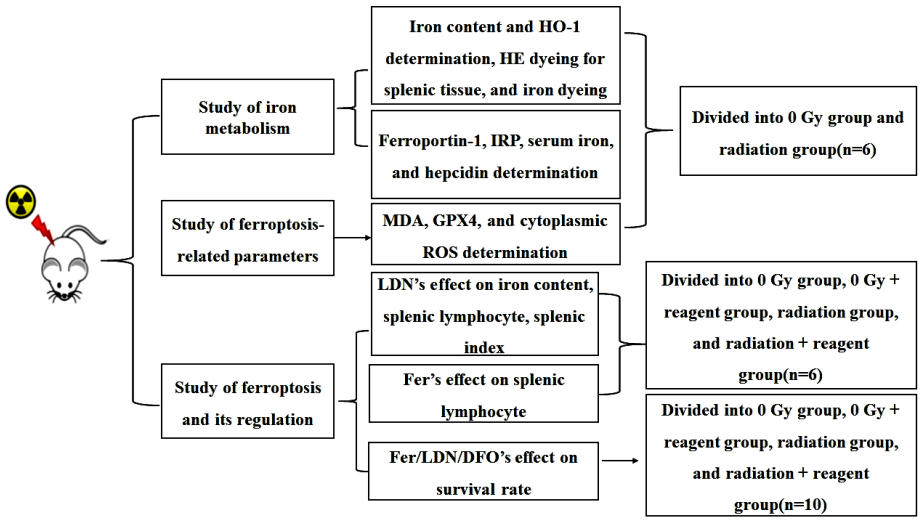


Figure 1. A schematic diagram for groups. HE: hematoxylin and eosin, HO-1: heme oxygenase-1, IRP: iron regulatory protein, MDA: malondialdehyde, GPX4: glutathione peroxidase 4, LDN: LDN193189, Fer: ferrostatin 1, DFO: deferoxamine.

[Downloaded from ijrr.com on 2026-11-10]
[DOR: 20.1001.1.23223243.2021.19.1.12.3]
[DOI: 10.29252/ijrr.19.1.99]

Iron content in the spleen

The spleen was removed into pre-cold phosphate-buffered saline solution (PBS) immediately after the mice were anesthetized with pentobarbital (40 mg/kg; Nanjing Reagent Co., Nanjing, Jiangsu, China). The pre-cold spleen tissue was then homogenized. The supernatant was collected after the homogenate was centrifuged at 4°C with 3000 rpm/min for 20 min. The sediment of the homogenate was re-suspended and lysed with NP-40 lysate (Beyotime Co., Shanghai, China), and the supernatant was collected again. The two supernatants were mixed and determined with a flame atomic absorption spectrophotometer (Persee Co., Beijing, China) to evaluate the iron level of the spleen.

Histomorphological analysis

The spleen was fixed overnight in 4% paraformaldehyde. The fixed sample was dehydrated through a series of graded alcohols, cleared in xylene, embedded with paraffin, and serially sectioned. Sections were deparaffinized and stained with hematoxylin and eosin. An optical microscope (CX31, Olympus Optical Co., Tokyo, Japan) was used to observe the slide.

Enzyme-linked immunosorbent assay (Elisa) of HO-1, Iron regulatory protein (IRP), GPX4, and hepcidin

The supernatant collected from the homogenate of the pre-cold spleen tissue was measured with Elisa kits (BD Company, Franklin Lakes, NJ, and USA) to evaluate HO-1, IRP1, IRP2, and GPX4 of the spleen. For the measurement of hepcidin in serum, blood was collected from the orbital sinus of mice. Each blood sample was centrifuged after it was set aside at the room temperature for 30 min. The corresponding supernatant (serum) was used for hepcidin Elisa (BD Company) determination.

Prussian blue staining

The homogenate obtained from the pre-cold spleen tissue was smeared on a glass slide. A Prussian Blue Nucleus Fixation Kit (Jiancheng Bio., Nanjing, Jiangsu, China) was used to stain the iron in splenic cells according to the manufacturer's instructions. The optical microscope (Olympus Optical Co.) was used to observe the slide smearing with oil.

Western blotting of Ferroportin 1

The sediment of the homogenate of the pre-cold spleen tissue was lysed on ice with RIPA buffer containing 1 mM PMSF. The protein concentration of the cell lysate was determined with a BCA kit (Pierce, Rockford, IL, USA). The sample with 20 μg of protein was separated with 13% SDS-PAGE and transferred onto PVDF membranes. Primary antibody to detect ferroportin 1 (1:1000; Kerafast Inc., Boston, MA, USA) was incubated overnight with the membranes at 4°C and incubated with horseradish peroxidase-conjugated secondary antibody (1:5000) for 2 h. Ferroportin 1 was detected with an ECL kit (KeyGEN, Nanjing, Jiangsu, China). GAPDH served as the internal loading control. The gray level of each band was quantified using ImageJ (National Institutes of Health, Bethesda, MD, USA).

Serum iron assay

The serum was extracted and analyzed with a Serum Iron Detection Kit (Jiancheng Bio.) to evaluate the level of serum iron.

Lymphocyte viability assay

Lymphocytes were extracted from the homogenate of the pre-cold spleen tissue with lymphocyte separation medium (LTS 1092; Tianjin Haoyang Co., Tianjin, China). The viability of the lymphocyte was estimated using a CCK-8 Counting Kit (Beyotime Co.) according to the manufacturer's instructions.

Spleen index

Each mouse was weighed. The spleen of each mouse was removed and weighed. The spleen index was calculated as spleen weight/body weight.

Malondialdehyde (MDA) determination

The homogenate of the pre-cold spleen tissue was measured with a MDA Assay Kit (A003-1; Jiancheng Bio.) to evaluate the MDA level of the spleen according to manufacturer's instructions.

[Downloaded from ijrr.com on 2026-11-10]

[DOR: 20.1001.1.23223243.2021.19.1.12.3]

[DOI: 10.29252/ijrr.19.1.99]

Cytoplasmic ROS level analysis

The sediment of the homogenate of the pre-cold spleen tissue was washed with PBS and incubated with 2,7-dichlorodihydrofluorescein diacetate (DCFH-DA, 10 μM; Beyotime Co.) for 20 minutes in a 37 °C water bath. The cytoplasmic ROS level was evaluated by measuring the mean fluorescence intensity of DCFH-DA with the use of flow cytometry (BD Bioscience, San Jose, CA, USA; Chen *et al.* 2015).

Statistical analysis

All data were presented as mean ± SD. Significant differences between groups were evaluated with a one-way analysis of variance, followed by a post-hoc student-Newman-Keuls test for multiple comparisons. Survival rates were analyzed with the Kaplan-Meier method and the Log-Rank test. A *p*-value less than 0.05 was considered statistically significant.

RESULTS

Gamma radiation increases iron content of spleen

To examine the possible role of gamma radiation in raising iron content, we measured the iron content of spleen on days 0, 1, 3, 7, and 14 after mice were exposed to 4 or 8 Gy of gamma radiation. Compared with the control mice, the irradiated mice showed significant increase in their iron levels on day 3, which reached the maximum on day 7 (up to 0.62 g/g after 8 Gy of gamma radiation). The iron level decreased to the baseline level on day 14 (figure 2a). The data indicate that gamma radiation increases the iron content of spleen in mice. We then studied the mechanism of iron accumulation in the spleen of irradiated mice. Haematoxylin and eosin staining exhibited a large number of erythrocytes in the spleen tissue on the first, third, and seventh days after mice were exposed to 4 or 8 Gy of gamma radiation (figure 2b). The histomorphological data indicate that gamma radiation caused bleeding in the spleen of the mice. We further measured the concentration of HO-1 in the spleen because the function of HO-1 is to decompose hemes into iron ions, biliverdin, and carbon monoxide, which may be one of the mechanisms underlying the iron accumulation. However, the concentration of HO-1 in the spleen significantly decreased on the first and third days post-irradiation (figure 2c). The depletion of HO-1 indicates decreased decomposition of hemes in macrophages, which suggests that iron accumulation is not primarily derived from the decomposition of hemes catalysed by HO-1. Prussian blue staining reflects the existence of haemosiderin, which is an iron granule formed by combination of the iron in haemoglobin with other proteins. The Prussian blue-positive area significantly increased on the third day post-irradiation (figure 2d), which indicates increased haemosiderin levels in the spleen of irradiated mice. These data together suggest that iron accumulation is primarily due to the increased haemosiderin formation resulting from radiation-induced bleeding in the spleen.

Gamma radiation alters iron metabolism in the spleen

To find a target for regulating iron accumulation in the spleen, we examined the iron metabolism of the spleen in gamma-irradiated mice. Ferroportin 1 is the only known transmembrane protein that transports iron from inside a cell to the bloodstream. When the cell contains a high-level of iron, IRP post-transcriptionally promotes the expression of ferroportin 1 to increase iron export. When serum iron levels increase, serum hepcidin levels will increase to reduce serum iron through the degradation of ferroportin 1. Ferroportin 1, IRP1, IRP2, hepcidin, and serum iron are, therefore, key elements for iron homeostasis in the body. We thus detected these five molecules on the seventh day after mice were exposed to gamma radiation. The irradiated mice showed an increase in expression of ferroportin 1 and decreases in IRP1 and IRP2 levels in the spleen (figure 3a-3c). These data indicate that the high iron in the spleen (figure 2a) decreases IRP1 and IRP2 to facilitate the expression of ferroportin 1, which promotes the iron export into the bloodstream.

[Downloaded from ijrr.com on 2026-11-10]
[DOR: 20.1001.1.23223243.2021.19.1.12.3]
[DOI: 10.29252/ijrr.19.1.99]

The irradiated mice also exhibited increased serum iron (up to 121.65 mmol/l; figure 3d). However, the concentration of hepcidin in the serum did not increase (figure 3e). These two data suggest that hepcidin did not exert its regulatory function on the serum iron in gamma -irradiated mice. The data of ferroportin 1, IRP1, IRP2, hepcidin, and serum iron together indicate that the high iron in the spleen induces an increase in the serum iron through activation of an IRP-ferroportin 1 axis; nevertheless, this increasing extent in the serum iron cannot trigger the hepcidin regulation on ferroportin 1. The lack of change in hepcidin level gives us a chance to regulate increased iron content in the spleen through the hepcidin target.

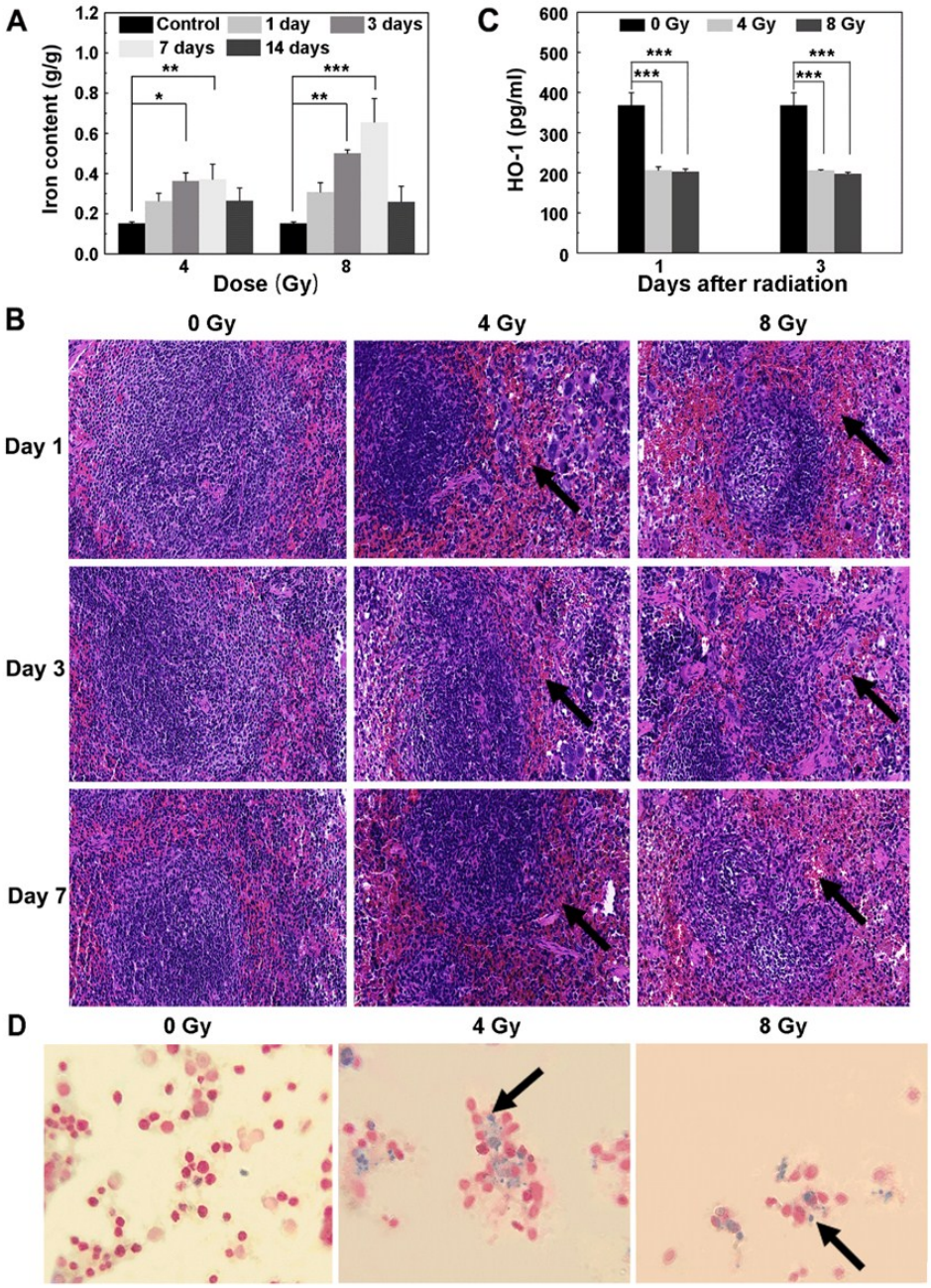


Figure 2. Gamma radiation induces iron accumulation in the spleen, which derives from increased haemosiderin formed due to haemorrhage in the spleen. Mice were exposed to 0/4/8 Gy of gamma radiation. Mice in the 0 Gy group were sham-irradiated. **(A)** Iron content of the spleen on days 0, 1, 3, 7, and 14 after being exposed to gamma radiation. **(B)** Hematoxylin and eosin-stained spleen (× 20) on days 0, 1, 3, and 7 after being exposed to gamma radiation. The black arrow points to erythrocytes. **(C)** HO-1 concentration of the spleen on days 1 and 3 after being exposed to gamma radiation. **(E)** Prussian blue staining of splenic cells (× 100) on day 3 after being exposed to gamma radiation. The black arrow points to the Prussian blue-positive area. The data presented as mean ± SD (n = 6); * $p< 0.05$, ** $p< 0.01$, and *** $p< 0.001$.

[Downloaded from ijrr.com on 2026-11-10]
[DOR: 20.1001.1.23223243.2021.19.1.12.3]
[DOI: 10.29252/ijrr.19.1.99]

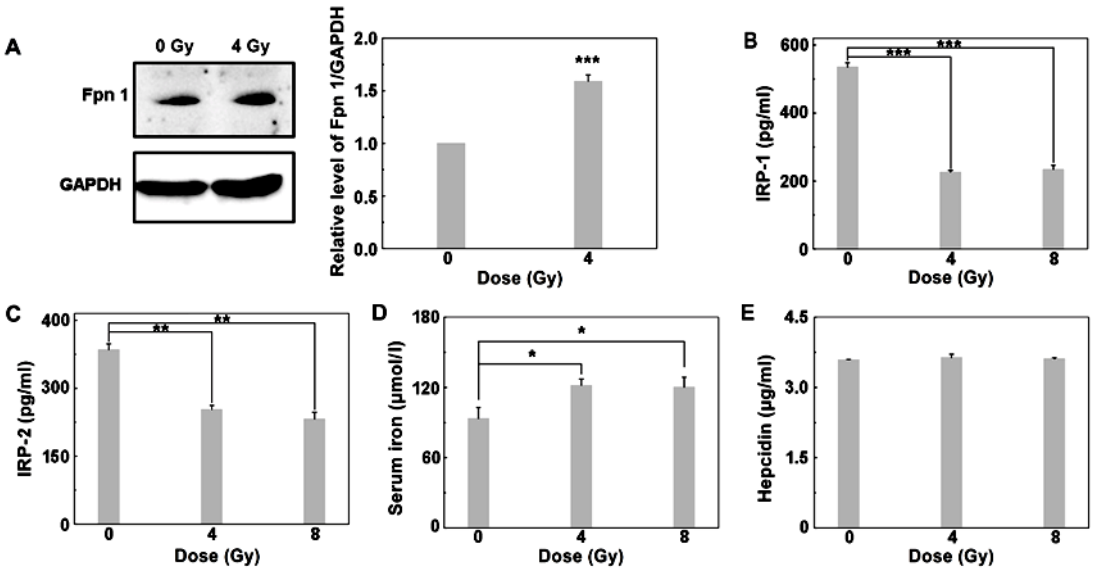


Figure 3. Gamma radiation alters iron metabolism of the spleen. Mice received 0/4/8 Gy of gamma radiation. Mice in the 0 Gy group were sham-irradiated. **(A)** Ferroportin-1 of the spleen on the seventh day post-irradiation. Fpn 1: Ferroportin-1 **(B)** Iron regulatory protein 1 of the spleen on the seventh day post-irradiation. IRP1: Iron regulatory protein 1 **(C)** Iron regulatory protein 2 of the spleen on the seventh day post-irradiation. IRP 2: Iron regulatory protein 2 **(D)** Serum iron on the seventh day post-irradiation. **(D)** Serum hepcidin on the seventh day post-irradiation. The data presented as mean ± SD (n = 6); * p< 0.05, ** p< 0.01, and *** p< 0.001.

Iron accumulation decreases viability of lymphocytes in the spleen

Based on our data of unchanged serum hepcidin level in gamma-irradiated mice, we chose LDN193189, an inhibitor of activin receptor-like kinase-2 (ALK2) and ALK3 that promotes hepcidin expression [26], to regulate the iron content of the spleen. We injected LDN193189 intraperitoneally into gamma-irradiated mice and measured iron content of the spleen on the first, and fifth days after LDN193189 treatment. The mice exposed to gamma radiation and LDN193189 showed a significant decrease in the iron content of the spleen (figure 4a). The data indicate that LDN193189 treatment decreases the iron content of the spleen effectively in gamma-irradiated mice.

Lymphocytes are major immune cells in the spleen, which closely relates to the immune function of the body. We then studied the effect of iron accumulation on splenic lymphocytes in irradiated mice with the use of LDN193189. The viability of splenic lymphocytes was measured 24 h after LDN193189 was injected into irradiated mice. LDN193189 mitigated the decrease in splenic lymphocytes of irradiated mice (figure 4b). Hematoxylin and eosin staining also exhibited an alleviation in the decrease of splenic lymphocytes 24 h after irradiated mice received LDN193189 (figure 4c). The data suggest that gamma radiation-induced iron accumulation causes a decrease in splenic lymphocytes. Besides, LDN193189 attenuated the decrease in the spleen index of irradiated mice (figure 4d). The data further support that iron accumulation decreases splenic lymphocytes in irradiated mice.

Iron accumulation induces ferroptotic cell death in splenic lymphocytes

We further ascertained whether ferroptosis exists in splenic lymphocytes of irradiated mice with the use of Ferrostatin-1, a ferroptotic inhibitor based on the alleviation of iron-induced lipid peroxidation. The viability of splenic lymphocytes was measured 24 h after Ferrostatin-1 was injected into gamma-irradiated mice. Ferrostatin-1 mitigated the decrease in the viability of splenic lymphocytes significantly in irradiated mice (figure 5a). The mice treated with gamma

[Downloaded from ijrr.com on 2026-11-10]
[DOR: 20.1001.1.23223243.2021.19.1.12.3]
[DOI: 10.29252/ijrr.19.1.99]

radiation and Ferrostatin-1 also exhibited increased lymphocytes in the white pulp of the spleen (figure 5b). Collectively, these data suggest that ferroptosis exists in splenic lymphocytes of irradiated mice.

To further support that ferroptosis exists in splenic lymphocytes, ferroptosis-related parameters of MDA, cytoplasmic ROS, and GPX4 in the spleen were measured on the third day after mice were exposed to 4 or 8 Gy of gamma radiation. The concentration of MDA increased (figure 5c) and GPX4 decreased (figure 5d). The results suggest that the increase in lipid peroxidation and the attenuation in alleviating lipid peroxidation occur in the spleen of irradiated mice. Cytoplasmic ROS has been reported to increase in erastin-induced ferroptosis [21]. Therefore, the cytoplasmic ROS was also measured. The cytoplasmic ROS in the spleen increased significantly on the third day post-irradiation (figure 5e). The changes in MDA, cytoplasmic ROS, and GPX4 support that ferroptosis exists in the splenic lymphocytes of irradiated mice.

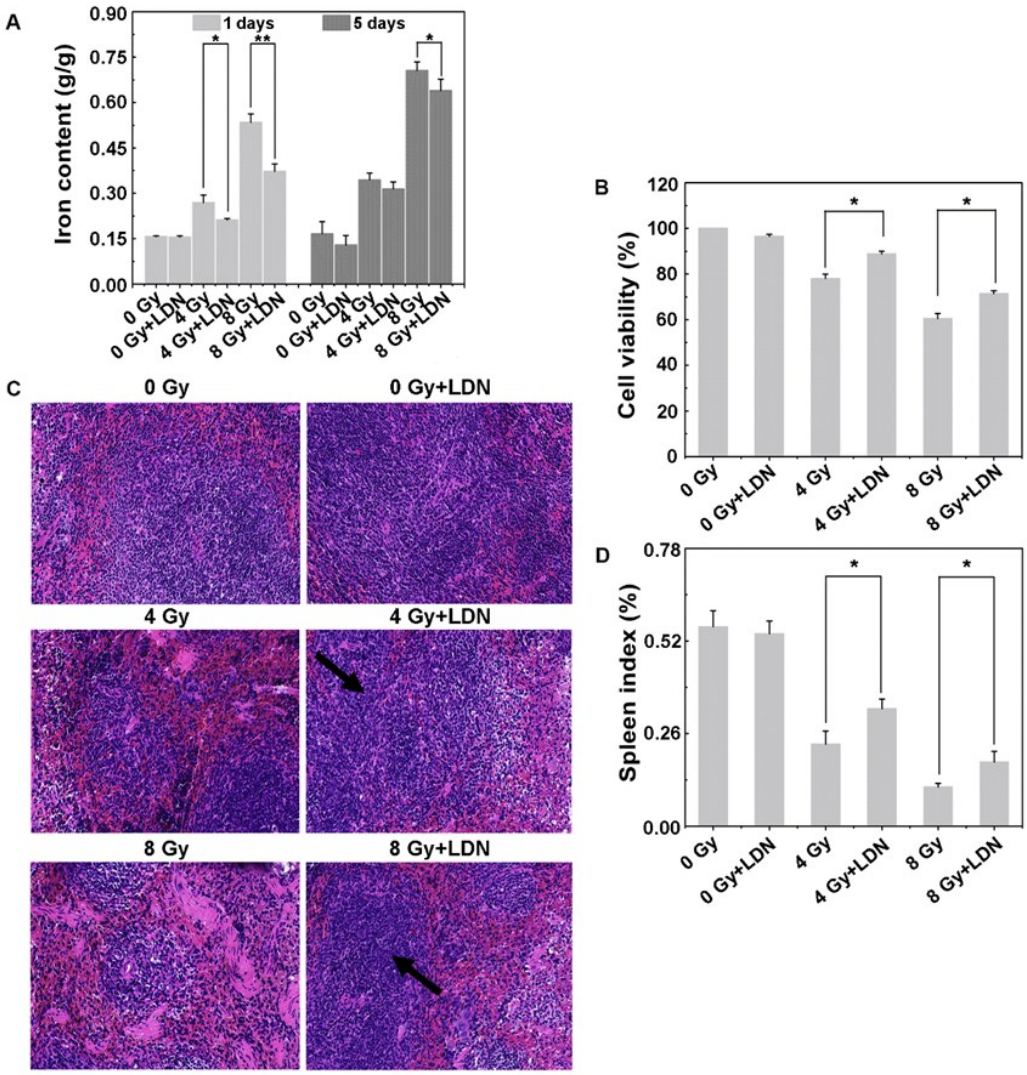


Figure 4. Regulatory effect of LDN193189 on iron content and splenic lymphocytes of irradiated mice. Mice were treated with LDN193189 (3 mg/kg) at 24 and 48 h postirradiation. Mice in the 0 Gy group or 0 Gy + LDN193189 group were sham-irradiated. **(A)** Iron content of the spleen on days 1 and 5 after LDN193189 was injected into irradiated mice. **(B)** Viability of splenic lymphocytes 24 h after LDN193189 was injected into irradiated mice. **(C)** Hematoxylin and eosin-stained spleen (× 20) 24 h after LDN193189 was injected into irradiated mice. The black arrow points to lymphocytes in the white pulp. **(D)** Spleen index 24 h after LDN193189 was injected into irradiated mice. LDN: LDN193189.The data presented as mean ± SD (n = 6); *p< 0.05, and **p< 0.01.

[Downloaded from ijrr.com on 2026-11-10]
[DOR: 20.1001.1.23223243.2021.19.1.12.3]
[DOI: 10.29252/ijrr.19.1.99]

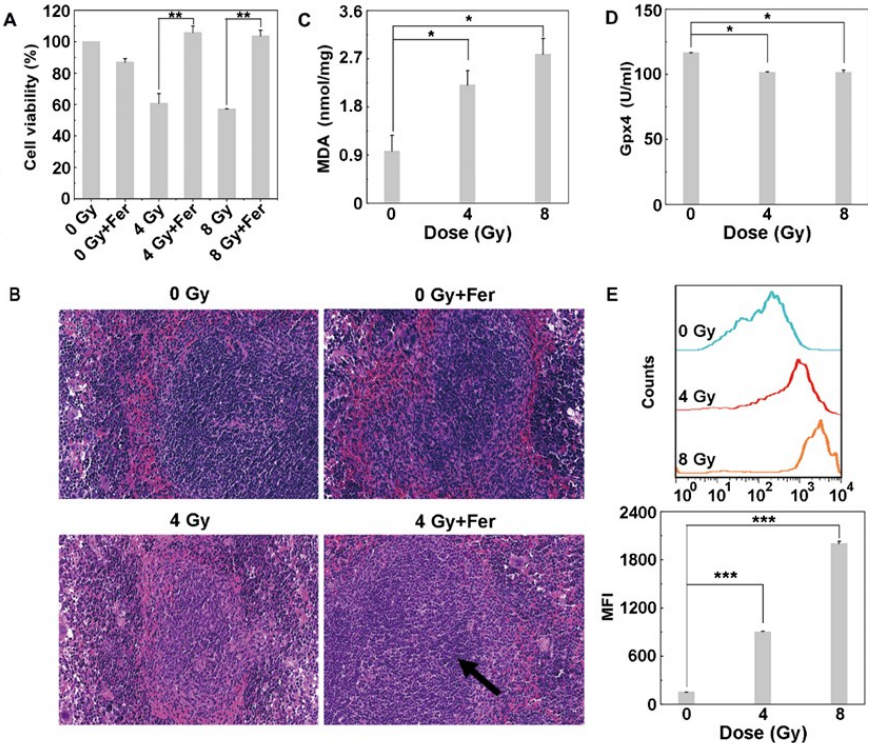


Figure 5. Ferroptosis occurs in splenic lymphocytes of irradiated mice. Mice in the 0 Gy group or 0 Gy + reagent group were sham-irradiated. **(A)** Viability of splenic lymphocytes 24 h after Ferrostatin-1 was injected into irradiated mice. Mice were treated with Ferrostatin-1 (2 mg/kg) 72 h after being exposed to 4 or 8 Gy of gamma radiation. Fer: Ferrostatin 1 **(B)** Hematoxylin and eosin-stained spleen (× 20) 24 h after Ferrostatin-1 was injected into irradiated mice. The black arrow points to lymphocytes in the white pulp. Mice were treated with Ferrostatin-1 (2 mg/kg) 72 h after being exposed to 4 Gy of gamma radiation. Fer: Ferrostatin 1. **(C)** MDA of the spleen tissue on the third day after mice were exposed to 4 or 8 Gy of gamma radiation. **(D)** GPX4 of the spleen tissue on the third day after mice were exposed to 4 or 8 Gy of gamma radiation. **(E)** Cytoplasmic ROS of the spleen tissue on the third day after mice were exposed to 4 or 8 Gy of gamma radiation. MFI: Mean fluorescence intensity. The data presented as mean ± SD (n = 6); * p< 0.05, ** p< 0.01, and *** p< 0.001.

Inhibition of ferroptosis improves survival of irradiated mice

Ferrostatin-1 and LDN193189 were used to study their ability in the improvement of the survival rate of irradiated mice. We monitored the survival rate of Ferrostatin-1/ LDN193189 combined with 10 Gy of gamma radiation for 120 days. The survival rate Ferrostatin-1 combined with 10 Gy of gamma radiation was 60% (Figure 6a), and LDN193189 combined with 10 Gy of gamma radiation was 40% (figure 6b). As DFO has been reported to inhibit ferroptosis [25], we also studied DFO's ability in the improvement of the survival rate of irradiated mice. Irradiated mice treated with DFO showed a 20% survival rate for 120 days. However, this survival rate was not significantly different from that of the irradiated mice without treatment (figure 6c). These data suggest that inhibition of ferroptosis through the decrease of iron-mediated ROS (Ferrostatin-1) or iron contents (LDN193189) could improve the survival rate of irradiated mice.

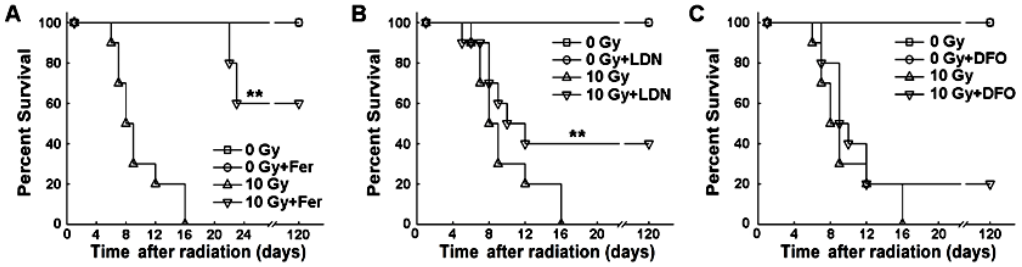


Figure 6. Inhibition of ferroptosis increases the survival rate of irradiated mice (10 Gy). **(A)** Survival rates after Ferrostatin-1 was injected into irradiated mice. Mice were treated with Ferrostatin-1 (2 mg/kg) 72 h after being exposed to 10 Gy of gamma radiation. Fer: Ferrostation-1. **(B)** Survival rates after LDN193189 was injected into irradiated mice. Mice were treated with LDN193189 (3 mg/kg) at time points of 24 and 48 h after being exposed to 10 Gy of gamma radiation. LDN: LDN193189. **(C)** Survival rates after DFO was injected into irradiated mice. Mice were treated with DFO (210 mg/kg) on days 1, 2, 3, 4, 5, and 6 after being exposed to 10 Gy of gamma radiation. Kaplan-Meier analysis was used (n = 10); ** p< 0.01 vs 10 Gy group.

[Downloaded from ijrr.com on 2026-11-10]
[DOR: 20.1001.1.23223243.2021.19.1.12.3]
[DOI: 10.29252/ijrr.19.1.99]

DISCUSSION

Ferroptosis is a form of cell death driven by iron-mediated lipid peroxidation and the Fenton reaction. In this study, we demonstrated that gamma radiation induces haemorrhage-based haemosiderin-related iron accumulation in the spleen, and this iron accumulation causes ferroptosis in splenic lymphocytes of mice.

Haemorrhage is one of the early signs of hematopoietic acute radiation sickness, due to increased permeability of vessel walls. Increased haemorrhage-based haemosiderin in the spleen in turn induced changes in iron metabolism. Increased Ferroportin 1 and decreased IRP1 and IRP2 levels (figure 3a-3c) suggest that the IRP-ferroportin 1 axis has been triggered to promote the expression of ferroportin 1 to facilitate iron transfer from the spleen to the bloodstream, which resulted in increased serum iron level (figure 3c). Nevertheless, the increased serum iron level did not induce increase in serum hepcidin level in irradiated mice (figure 3d), which indicates that the hepcidin-ferroportin 1 axis was not triggered. The inactivation of the hepcidin-ferroportin 1 axis indicates that ferroportin 1 cannot be degraded by hepcidin, which is also in favour of iron transfer from the spleen to the bloodstream. Therefore, to recover the iron homeostasis of the spleen after radiation, the IRP-ferroportin 1 axis took precedence over the hepcidin-ferroportin 1 axis. Dixon et al. identified *IREB8*, which codes for IRP2, as the high-confidence gene for erastin-induced ferroptosis in HT-1080 and Calu-1 cells [21]. However, IRP2 level decreased upon radiation-induced ferroptosis in splenic lymphocytes. This phenomenon may be attributed to the different mechanisms of these two types of ferroptosis. The former is through inactivation of the major protective mechanism of the membrane against peroxidation damage, and the latter is iron-related which causes imbalance in iron metabolism.

Given increased haemosiderin and altered iron metabolism in the spleen, we think that although the expression of ferroportin 1 increased, it was not sufficient to help iron ions in the spleen being transported into the bloodstream in a short period. Therefore, haemorrhage-based haemosiderin-related iron accumulation of the spleen occurred up to 7 days after mice were exposed to gamma radiation (figure 2a, 2b, and 2d).

Iron accumulation induced by brain haemorrhage has been studied extensively [27, 28]. This kind of iron accumulation accompanied by increased HO-1 level differs from radiation-induced haemorrhage-based iron accumulation in the spleen that is accompanied by decreased HO-1 level (figure 2c). HO-1 is the key enzyme for decomposition of heme into iron ions. The difference between changes in HO-1 concentration suggests the different mechanisms in radiation-induced and brain injury-induced iron accumulation. Radiation-induced iron accumulation is due to the formation of haemosiderin (figure 2d), and brain injury-induced iron accumulation may be due to iron ions decomposed from hemes.

Using LDN193189, we demonstrated that gamma radiation-induced iron accumulation decreased the viability of splenic lymphocytes in mice (figure 4b and 4c). Further, using the ferroptosis inhibitor (figure 5a and 5b) and measuring ferroptosis-related parameters, we demonstrated that ferroptosis occured in splenic lymphocytes (figure 2a, and figure 5c-5e). Lymphocytes are the only radiosensitive mature blood cells, and lymphocyte-mediated specific immunity is the second line of defence in the immune system. Radiation-induced ferroptosis in splenic lymphocytes, therefore, contributes to infection presented in hematopoietic acute radiation sickness. This kind of ferroptosis is based on haemosiderin-related iron accumulation caused by gamma radiation-induced haemorrhage in the spleen tissue. Ferroptosis is also found in neurons after an intracerebral haemorrhage occurs in mice [29]. These data suggest a direct relationship between severe organ haemorrhage and ferroptosis, which suggests that we should take precautionary measures to prevent ferroptosis when severe haemorrhagic disease occurs.

The non-canonical ferroptosis induction is

[Downloaded from ijrr.com on 2026-11-10]
[DOR: 20.1001.1.23223243.2021.19.1.12.3]
[DOI: 10.29252/ijrr.19.1.99]

iron-related [20]. Radiation-induced ferroptosis in splenic lymphocytes caused by haemosiderin-related iron. Therefore, radiation-induced ferroptosis in splenic lymphocytes is the non-canonical ferroptosis induction. LIP serves as the initial trigger of ferroptosis [30]. The mechanism of haemosiderin-induced ferroptosis is not clear. Did haemosiderin directly induce ferroptosis or it induce ferroptosis after it transforms into the LIP (there is a pathway in the transformation of haemosiderin into the LIP in iron mobilization [31])? The mechanism of haemosiderin in the trigger of ferroptosis warrants further studies.

HO-1 serves a dominant role in ferroptosis because it is a regulator not only in iron homeostasis but also in ROS homeostasis [32-34]. However, the effect of HO-1 in the regulation of ferroptosis remains dual. When HO-1 moderately activates, nuclear factor erythroid 2-related factor 2-derived HO-1 exerts an anti-ferroptosis effect by neutralizing ROS [22, 35, 36]. When expressed at a higher level, HO-1 exhibits pro-ferroptosis force through the increase of iron ion, and generation of iron-mediated ROS overload [37, 38]. In this study, HO-1 concentration decreased in the spleen of irradiated mice (figure 2c), which suggests that HO-1 did not involve in iron accumulation and ROS reaction during ferroptosis in splenic lymphocytes. Thus, the mechanism of gamma radiation-induced ferroptosis may be different from that of ferroptosis accompanied by a high-level of HO-1. This speculation needs further exploration.

Ferrostatin-1 or LDN193189 treatment significantly improved the survival rate of irradiated mice (figure 6a and 6b), which suggests that alleviating the decrease in splenic lymphocyte count improves the survival rate of irradiated mice. These improvements also indicate that ferroptosis is a significant form of gamma radiation-induced cell death in splenic lymphocytes.

Ferrostatin-1 inhibits ferroptosis through decrease in iron-mediated lipid peroxidation, LDN193189 results in redistribution of iron ions from tissue to the bloodstream, and DFO chelates iron ions. Among these three ferroptosis inhibitors, Ferrostatin-1treatment elicited the best improvement in the survival rate of irradiated mice, followed by treatment with LDN193189, and finally with DFO (figure 6). These data have two implications. One is that iron-mediated lipid peroxidation is essential for ferroptosis [39]. The other is that inhibiting ferroptosis through the regulation of iron content is a feasible strategy. LDN193189 treatment promotes the redistribution of iron from cells into the bloodstream through inhibition of hepcidin-mediated decomposition of ferroportin 1. DFO chelates iron ions in the bloodstream, and is excreted in the urine. The better performance of LDN193189 suggests that the redistribution of iron ions from the iron-accumulated organ to the bloodstream is more effective than chelation of iron ions and excreting them in the urine for the treatment of hematopoietic acute radiation sickness.

CONCULSIONS

Gamma radiation induces haemorrhage-based iron accumulation in the spleen of mice. This iron accumulation damages splenic lymphocytes through ferroptosis. The inhibition of ferroptosis improves the survival rate of irradiated mice. Further work should focus on the mechanism of ferroptosis in splenic lymphocytes induced by gamma radiation, which is a critical concern for discovery and development of agents that mitigate radiation injuries.

ACKNOWLEDGMENTS

This work was supported by the National Natural Science Foundation of China (Grant numbers 11575086, 11775115, 11705089, and 81571805), the Postdoctoral Science Foundation of China (Grant number 2017M611660), the Priority Academic Program Development of Jiangsu Higher Education Institutions.

***Conflicts of interest*:** *Declared none.*

[Downloaded from ijrr.com on 2026-11-10]

[DOR: 20.1001.1.23223243.2021.19.1.12.3]

[DOI: 10.29252/ijrr.19.1.99]

REFERENCES

1. Jiang DW, Wang QR, Shen XR, He Y, Qian TT, Liu Q, Hou DY, Liu MY, Chen W, Ren X, Li KX (2017) Radioprotective effects of cimetidine on rats irradiated by long-term, low-dose-rate neutrons and ^{60}Co-γ rays. *Mil Med Res, 4: 7*.
2. Yi LR, Tian M, Piao C, Gao G, Wu LN, Pan Y, Liu JX (2019) The protective effects of 1, 2-propanediol against radiation-induced hematopoietic injury in mice. *Biomed Pharmacother, **114(108806)**: 1-12*.
3. Zhou RF, Long HS, Zhang B, Lao ZZ, Zheng QY, Wang TC, Zhang YX, Wu QG, Lai XP, Li G, Lin LZ (2019) Salvianolic acid B, an antioxidant derived from Salvia militarize, protects mice against radiation-induced damage through Nrf2/Bach1. *Mol Med Rep, **19**: 1309-1317*.
4. Viklicky V and Trebichavsky I (1970) Effect of ionizing radiation on the frequency and ultrastructure of mast cells in mouse spleen. *Folia Biol, **16(5)**: 347-352*.
5. Makinodan T, Nettesheim P, Morita T, Chadwick CJ (1967) Synthesis of antibody by spleen cells after exposure to kiloroentgen doses of ionizing radiation. *J Cell Physiol, **69 (3)**: 355-366*.
6. Baker WH, Limanni A, Chang CM, Jackson WE, Seemann R, Patchen ML (1995) Comparison of interleukin-1 alpha gene expression and protein levels in the murine spleen after lethal and sublethal total-body irradiation. *Radiat Res, **143(3)**: 320-326*.
7. Ishihara H, Tsuneoka K, Dimchev AB, Shikita M (1993) Induction of the expression of the interleukin-1 beta gene in mouse spleen by ionizing radiation. *Radiat Res, **133(3)**: 321-326*.
8. Holl V, Coelho D, Weltin D, Defour P, Denis J, Florentin I, Mathieu J, Gueulette J, Bischoff P (2001) Induction of apoptosis in murione splenic lymphocytes using carbon ion beam. *Can J Physiol Pharmacol, **79(2)**: 109-113*.
9. Smina TP, De S, Devasagayam TPA, Adhikari S, Janardhanan KK (2011) Ganoderma lucidum total triterpenes prevent radiation-induced DNA damage and apoptosis in splenic lymphocytes in vitro. *Mutat Res-Gen Tox En, **726(2)**: 188-194*.
10. Kondo T (2013) Radiation-induced cell death and its mechanisms. *Radiat Emerg Med, **2**: 1-4*.
11. Aisen P, Enns C, Wessling-Resnick M (2001) Chemistry and biology of eukaryotic iron metabolism. *Int J Biochem Cell Biol, **33**: 940-959*.
12. Bogdan AR, Miyazawa M, Hashimoto K, Tsuji Y (2016) Regulators of iron homeostasis: New players in metabolism, cell death, and disease. *Trends Biochem Sci, **41**: 274-286*.
13. Eid R, Arab NTT, Greenwood MT (2017) Iron mediated toxicity and programmed cell death: A review and a re-examination of existing paradigms. *BBA-Mol Cell Res, **1864**: 399-430*.
14. Shintoku R, Takigawa Y, Yamada K, Kubota C, Yoshimoto Y, Takeuchi T, Koshiishi I, Torii S (2017) Lipoxygenase-mediated generation of lipid peroxides enhances ferroptosis induced by erastin and RSL3. *Cancer Sci, **108**: 2187-2194*.
15. Cheng J, Fan YQ, Liu BH, Zhou H, Wang JM, Chen QX (2020) ACSL4 suppresses glioma cells proliferation via activating ferroptosis. *Oncol Rep*, ***43**: 147-158*.
16. Gao M, Monian P, Quadri N, Ramasamy R, Jiang X (2015) Glutaminolysis and transferrin regulate ferroptosis. *Mol Cell, **59**: 298-308*.
17. Wu JR, Tuo QZ, Lei P (2018) Ferroptosis, a recent defined form of critical cell death in neurological disorders. *J Mol Neurosci, **66(2)**: 197-206*.
18. Xie Y, Hou W, Song X, Yu Y, Huang J, Sun X, Kang R, Tang D (2016) Ferroptosis: process and function. *Cell Death Differ, **23(3)**: 369-379*.
19. Wenzel SE, Tyurina YY, Zhao JM, St. Croix CM, Dar HH, Mao GW, Tyurin VA, Anthonymuthu TS, Kapralov AA, Amoscato AA, *et al.* (2017) PEBP1 wardens ferroptosis by enabling lipoxygenase generation of lipid death signals. *Cell*, ***171**: 628-641*.
20. Hassannia B, Vandenabeele P, Berghe TV (2019) Targeting ferroptosis to iron out cancer. *Cancer Cell*, ***35**: 830-849*.
21. Dixon SJ, Lemberg KM, Lamprecht MR, Skouta R, Zaitsev EM, Gleason CE, Patel DN, Bauer AJ, Cantley AM, Yang WS, Morrison B, Stockwell BR (2012) Ferroptosis: An iron-dependent form of nonapoptotic cell death. *Cell, **149**: 1060-1072*.
22. Chiang SK, Chen SE, Chang LC (2018) A dual role of heme oxygenase-1 in cancer cells. *Int J Mol Sci, **20**(1): E39*.
23. Lee YC, Cheng CJ, Bilen MA, Lu JF, Satcher RL, Yu-Lee LY, Gallick GE, Maity SN, Lin SH (2011) BMP4 promotes prostate tumor growth in bone through in bone through osteogenesis. *Cancer Res, **71**(15): 5194-5203*.
24. Sui SY, Zhang J, Xu SP, Wang Q, Wang PY, Pang D (2019) Ferritinophagy is required for the induction of ferroptosis by the bromodomain protein BRD4 inhibitor(+)-JQ1 in cancer cells. *Cell Death Dis, **10**: 331*.
25. Yao X, Zhang Y, Hao J, Duan HQ, Zhao CX, Sun C, Li B, Fan BY, Wang X, Li WX, Fu XH, Hu Y, Liu C, Kong XH, Feng SQ (2019) Deferoxamine promotes recovery of traumatic spinal cord injury by inhibiting ferroptosis. *Neural Regen Res, **14**(6):1068*.
26. Yu PB, Deng DY, Lai CS, Hong CC, Cuny GD, Bouxsein ML, Hong DW, McManus PM, Katagiri T, Sachidanandan C, Kamiya N, Fukuda T, Mishina YJ, Peterson RT, Bloch KD (2008) BMP type I receptor inhibition reduces heterotopic ossification. *Nature Med*, ***14**: 1363-1369*.
27. Chen Z, Gao C, Hua Y, Keep RF, Muraszko K, Xi GH (2010) Role of iron in brain injury after intraventricular haemorrhage. *Stroke, **42**: 465-470*.
28. Wan S, Hua Y, Keep RF, Hoff JT, Xi G (2006) Deferoxamine reduces CSF free iron levels following intracerebral haemorrhage. *Acta Neurochir Suppl, **96**: 199-202*.
29. Li Q, Han XN, Lan X, Gao YF, Wan JR, Durham F, Cheng T, Yang J, Wang Z, Jiang C, Ying M, Koehler RC, Stockwell BR, Wang J (2017) Inhibition of neuronal ferroptosis protects hemorrhagic brain. *JCI Insight, **2**(7): e90777*.
30. Doll S and Conrad M (2017) Iron and ferroptosis: A still ill-defined liaison. *IUBMB Life,* 69: 423-434.
31. Saito H, Tomita A, Ohashi H, Maeda H, Hayashi H, Naoe T (2012) Determination of ferritin and haemosiderin iron in

[Downloaded from ijrr.com on 2026-11-10]

[DOR: 20.1001.1.23223243.2021.19.1.12.3]

[DOI: 10.29252/ijrr.19.1.99]

patients with normal iron strores and iron overload by serum ferritin kinetics. *Nagoya J Med Sci,* ***74****: 39-49*.
32. Abraham NG and Kappas A (2008) Pharmacological and clinical aspects of heme oxygenase. *Pharmacol Rev,* ***60****: 79 -127*.
33. Ryter SW, Alam J, Choi AM (2006) Heme oxygenase-1/ carbon monoxide: From basic science to therapeutic applications. *Physiol Rev,* ***86****: 583-650*.
34. Vitek L and Schwertner HA (2007) The heme catabolic pathway and its protective effects on oxidative stress-mediated diseases. *Adv Clin Chem,* ***43****: 1-57*.
35. Adedoyin O, Boddu R, Traylor A, Lever JM, Bolisetty S, George JF, Agarwal A (2018) Heme oxygenase-1 mitigates ferroptosis in renal proximal tubule cells. *Am J Physiol Renal Physiol,* ***314****: F702-F714*.
36. Sun XF, Ou ZH, Chen RC, Niu XH, Chen D, Kang R, Tang DL (2016) Activation of the p62-Keap1-Nrf2 pathway protects against ferroptosis in hepatocellular carcinoma cells. *Hepatology,* ***63****: 173-184*.
37. Chang LC, Chiang SK, Chen SE, Yu YL, Chou RH, Chang WC (2018) Heme oxygenase-1 mediates BAY11-7085 induced ferroptosis. *Cancer Lett,* ***416****: 124-137*.
38. Sui M, Jiang XF, Chen J, Yang HY, Zhu Y(2018) Magnesium isoglycyrrhizinate ameliorates liver fibrosis and hepatic stellate cell activation by regulating ferroptosis signaling pathway. *Biomed Pharmacother,* ***106****: 125-133*.
39. Yang WS and Stockwell BR (2016) Ferroptosis: death by lipid peroxidation. *Trends cell Biol,* ***26****(3): 165-176*.

[Downloaded from ijrr.com on 2026-11-10]
[DOR: 20.1001.1.23223243.2021.19.1.12.3]
[DOI: 10.29252/ijrr.19.1.99]

[DOI: 10.29252/ijrr.19.1.99] [DOR: 20.1001.1.23223243.2021.19.1.12.3] [Downloaded from ijrr.com on 2026-11-10]